Since January 2020 Elsevier has created a COVID-19 resource centre with free information in English and Mandarin on the novel coronavirus COVID-19. The COVID-19 resource centre is hosted on Elsevier Connect, the company's public news and information website.

DNA Repair 94 (2020) 102899

Contents lists available at ScienceDirect

DNA Repair

journal homepage: www.elsevier.com/locate/dnarepair

Molecular basis for the MacroD1-mediated hydrolysis of ADP-ribosylation

Xiaoyun Yang[a,1], Yinliang Ma[a,1], Yimiao Li[a,1], Yating Dong[a,1], Lily L. Yu[b], Hong Wang[a], Lulin Guo[a], Chen Wu[a,*], Xiaochun Yu[c,*], Xiuhua Liu[a,*]

[a] College of Life Science, Institute of Life Science and Green Development, Hebei University, Baoding, 071000, Hebei, PR China
[b] Westridge School, 324 Madeline Dr., Pasadena, CA, 91105, USA
[c] Life Science Institute, Westlake University, Hangzhou, Zhejiang, PR China

ARTICLE INFO

Keywords:
DNA damage repair
ADP-ribosylation
MacroD1
ADPR
Crystal structure

ABSTRACT

MacroD1 is an enzyme that hydrolyzes protein mono-ADP-ribosylation. However, the key catalytic residues of MacroD1 in these biochemical reactions remain elusive. Here, we present the crystal structure of MacroD1 in a complex with ADP-ribose (ADPR). The β5-α10-loop functions as a switch loop to mediate substrate recognition and right orientation. The conserved Phe^{272} in the β5-α10-loop plays a crucial role in the orientation of ADPR distal ribose, and a conserved hydrogen-bond network contributes significantly to hold and orient the catalytic water12, which mediates ADPR hydrolysis. Moreover, we found that MacroD1 was recruited to the sites of DNA damage via recognition of ADP-ribosylation at DNA lesions. The MacroD1-mediated ADPR hydrolysis is essential for DNA damage repair. Taken together, our study provides structural and functional insights into the molecular mechanism of MacroD1-mediated ADPR hydrolysis and its role in DNA damage repair.

1. Introduction

Protein ADP-ribosylation is an important post-translational modification (PTM) that occurs in multiple biological processes, such as DNA damage repair [1,2]. A family of enzymes, named poly (ADP-ribose) polymerases (PARPs), use NAD^+ as a substrate to transfer ADP-ribose (ADPR) moieties onto proteins with two different forms, namely mono(ADP-ribosyl)ation (aka MARylation) and poly(ADP-ribosyl)ation (aka PARylation) [3,4]. To date, 17 PARPs have been identified in human cells. These enzymes use lysine, aspartate, glutamate, serine and cysteine as common acceptors, and covalently link them with ADPR via N-, O-, or S-glycosidic bonds [5,6].

Protein ADP-ribosylation and hydrolyzation of ADPR from its acceptor residue are in a reversible and dynamically regulated process, and several hydrolases have been reported to hydrolyze MARylation and PARylation [7,8]. In mammals, ADPR hydrolases can be categorized into two groups based on the enzymatic domain folding [1]: the DraG-like fold hydrolases [2]; the macro domain hydrolases [9]. Some DraG-like fold hydrolases have been well characterized, such as ARH1 and ARH3. ARH3 has been shown to hydrolyze poly-ADP-ribose (PAR) chains [10,11]. More recently, it has been proven to efficiently remove mono (ADP-ribose) (MAR) from serine residue [12]. ARH1 is the first DraG-like fold hydrolase found to hydrolyze MAR, and releases ADPR from arginine residue [13].

The macro domain is an evolutionarily conserved protein fold found in all kingdom of life [14,15]. Originally, macro domain has been found as an ADPR-binding motif [16]. Interestingly, a set of macro domain is known to digest ADP-ribosylation. PARG, MacroD1, MacroD2 and TARG1 are the most well characterized macro domain hydrolases. Although these proteins belong to the same family, they digest different substrates with distinct molecular mechanisms [2]. PARG is known to rapidly digest PAR chains by hydrolyzing the O-glycosidic bond between ADPR units, but is unable to hydrolyze the terminal ADPR unit linked directly to target proteins [17–20]. Thus, it cannot digest MAR. In contrast, MacroD1, MacroD2 and TARG1 are able to release ADPR from aspartic acid and glutamic acid residues [21–26].

Among these macro domain ADPR hydrolases, *human* MacroD1, MacroD2, *Escherichia coli* YmdB and *Trypanosoma brucei gambiense* TbMDO share similar structure and form a subgroup within the macro domain family enzymes, termed MacroD-like proteins [21,22,27,28].

Abbreviations: MAR, mono-ADP-ribosylation; OAADPr, 2-O-Acetyl-ADP-ribose; ADPR, ADP-ribose; PARPs, poly (ADP-ribose) polymerases; PTM, post-translational modification; RMSD, root mean square deviation; ARH, ADP-ribosylhydrolase; IPTG, isopropyl β-D-1-thiogalactopyranoside; MMS, methyl methanesulfonate; SSB, DNA single-strand break; DSB, DNA double-strand break

* Corresponding authors.
E-mail addresses: dawnwuchen@163.com (C. Wu), yuxiaochun@westlake.edu.cn (X. Yu), liuxiuhua_2004@163.com (X. Liu).
[1] X.Y., Y.M., Y.L. and Y.D. contribute equally.

https://doi.org/10.1016/j.dnarep.2020.102899
Received 7 May 2020; Received in revised form 9 June 2020; Accepted 11 June 2020
Available online 22 June 2020

These enzymes are able to hydrolyze not only ADPR but also 2-O-acetyl-ADP-ribose (OAADPr), a by-product of sirtuin-mediated protein deacetylation [22]. The crystal structure of MacroD1 (residues 91-325), the founding member of the MacroD-like proteins, has been solved and consists of an N-terminal region (residues 91-136) and a macro domain (residues 141-322) (21). The macro domain comprises of a three-layered α-β-α sandwich with a central six-stranded β-sheet. A possible substrate-binding mode was proposed using structure modeling, in which several conserved residues, such as Asn^{174}, Asp^{184} and His^{188}, are essential for catalytic activity of the deacetylation of OAADPr [21,29]. However, the detail substrate binding and catalytic mechanism underlying the MacroD1-mediated ADPR hydrolysis have not been examined.

It has been shown that protein ADP-ribosylation plays a key role in DNA damage repair [7,8]. It occurs quickly at DNA lesions and mediates the recruitment of DNA damage repair factors to DNA lesions via ADPR recognition for early phase DNA repair [7]. The biological functions of ADPR hydrolysis have also been studied in the context of DNA damage repair. Loss of dePARylation or deMARylation enzymes suppresses various types of DNA damage repair. Once DNA damage occurs, these enzymes can be recruited to DNA lesions quickly [8,30]. One possible explanation is ADPR hydrolysis releases DNA repair factors from repaired sites, so that these DNA repair factors can be recycled to repair other lesions. If ADPR hydrolysis is suppressed, ADPR-binding DNA repair factors will be trapped at DNA lesions, which suppresses DNA damage repair. Thus, it has been shown that PARG is involved in both DNA single-strand break (SSB) repair and double-strand break (DSB) repair [8,31]. TARG1 and ARH3 are also known to participate in SSB repair [8]. However, the role of MacroD1 in DNA damage repair has not been studied yet. Although it has been shown that an N-terminal-truncated isoform of MacroD1 (residues N78-C325) localizes in mitochondria, alternatively the full-length isoform of MacroD1 (residues N1-C325) localizes in nucleus, especially under cellular stress, indicating that MacroD1 may play roles in multiple biological processes [9,32].

To understand the molecular mechanism of MacroD1-mediated ADPR hydrolysis, we determined the crystal structure of MacroD1 in a complex with ADPR. Our analyses reveal the detailed catalytic pocket of MacroD1 and shed light on its ADPR recognition and the molecular mechanism of ADPR hydrolysis. Moreover, our results demonstrate that MacroD1 is recruited to DNA lesions through the ADP-ribosylation recognition, and MacroD1-mediated ADPR hydrolysis plays a critical role in DNA damage repair. Based on the structural analyses, we characterized the key residues of MacroD1 that are involved in DNA damage repair.

2. Results

2.1. Overall structure of MacroD1-ADPR complex

To understand the catalytic mechanism of MacroD1, we determined the structure of the MacroD1-ADPR complex to 2.0 Å resolution using X-ray diffraction. The final model of the MacroD1-ADPR complex contains four protein molecules in the asymmetric unit, termed A, B, C and D respectively. The electron density map shows that MacroD1 monomer binds to one ADPR molecule. The root mean square deviation (RMSD) between MacroD1 molecule A, B and C is less than 0.1 Å, revealing that the three MacroD1 molecules in the complex have nearly identical structure. The RMSD between molecule D and the other three is approximately 0.35 Å, which is mainly caused by the relative poor electron density of Molecule D. The MacroD1 molecule A combined with the ADPR ligand was used for the following structural analysis.

The MacroD1 monomer exhibits the canonical three-layered α-β-α sandwich with a central six-stranded β sheet containing a mixture of anti-parallel (β3-β4) and parallel (β2-β5-β6-β1) strands (Fig. 1A). The ADPR molecule binds to the deep cleft of MacroD1 according to the 2*Fo-Fc* electron density map (Fig. 1B). Structural alignment using the DALI server reveals the presence of many structural homologs of MacroD1 (Fig. 1C and D). The closest homolog is MacroD2 in complex with ADPR from *Homo sapiens* (PDB code: 4IQY, Z score of 36.5), giving a RMSD value of 1.3 Å for their corresponding Cα atoms. Additionally, MacroD1 also shares a similar structure with other macro domain-containing proteins, such as GDAP2 from *Homo sapiens* (PDB code: 4UML, Z score of 30.3, RMSD: 1.4 Å), TbMDO in complex with ADPR from *Trypanosoma brucei gambiense* (PDB codes: 5FSY and 5FSX; Z-score: 28.8 and 28.5 respectively; RMSD: 2.1 Å and 2.3 Å respectively) and YmdB from *Escherichia coli* (PDB code: 5CB5 and 5CB3, Z score: 26.7 and 26.5 respectively, RMSD: 1.0 Å and 1.1 Å respectively) (Fig. 1D). All these proteins share common macro domain fold, which contains a three-layered α-β-α sandwich, and their ADPR molecules exhibit a similar conformation (Fig. 1D and E). Notably, the conformation of these macro domains are remarkably different from that of the ADP-ribosylhydrolase (ARH) family enzymes, including ARH1 (PDB code: 6IUX), DraG (PDB code: 2WOC) and ARH3 (PDB code: 5ZQY), which represent a compact all-α-helical fold.

2.2. Conformational switches of MacroD1 enable specific substrate recognition

Compared to apo-MacroD1 (PDB code: 2X47), the most distinctive structural characteristic in the MacroD1-ADPR complex is the dramatic conformational change of the β5-α10-loop (Fig. 2A). The loop covering the bound ADPR functions as a switch loop to sequester substrate and provides structural flexibility to accommodate alternative substrates (Fig. 2A). Thus, the results suggest that the β5-α10-loop exists in two different states: open and closed states. The closed form will appear once ADPR binds to the open form (ligand-free state), which triggers a conformational change to rearrange the active site (Fig. 2E and F). Notably, this induced-fit movement mode causes the large displacement and rotation of residue Phe^{272} from the β5-α10-loop (approx. 8 Å, 100°) (Fig. 2B), which is incorporated into the catalytic site upon ADPR binding. Sequence alignment reveals that the corresponding residue for Phe^{272} in MacroD1-ADPR complex is Tyr in other macro domain hydrolases, such as Tyr^{190} in MacroD2, Tyr^{126} in YmdB and Tyr^{214} in TbMDO (Fig. 1C), indicating that the phenyl group is conserved in the macro domain hydrolase.

In addition, several conformational changes have been observed when ADPR binds to MacroD1. Val^{271} from the β5-α10-loop was moved towards to the catalytic site about ~ 7 Å (Fig. 2B), and Phe^{306} in β6-α11-loop undergoes a rotation to generate π-π stacking interaction with the adenine ring of ADPR (Fig. 2C). Another important conformational change is to form the glycine-rich β2-α7-loop once recognizing ADPR. It is the part of α7 helix in the ligand-free state (PDB code: 2X47). The helix-to-loop transition offers structural flexibility for the ADPR binding (Fig. 2D).

2.3. The structure of ADPR binding groove in MacroD1

ADPR is located at the deep substrate-binding groove of MacroD1. The ADPR molecule adopts an almost L-shaped conformation, and the long side consists of both pyrophosphate moiety and distal ribose of ADPR, and the adenosine moiety is loaded at the short side.

All the three parts of ADPR have extensive contacts with MacroD1 (Fig. 3A). The adenine ring in the adenosine forms hydrogen-bonds with the side-chain carbonyl oxygen of Asp^{160} and the main-chain amino group of Ile^{161}. Furthermore, the adenine ring is also stacked by Phe^{306} through the abovementioned π-π stacking interaction (Fig. 2C), which is a common characteristic for both macro domain hydrolases and ARH hydrolases [33]. The adenosine ribose forms hydrogen bonds with the side-chain of Thr^{269} and three water molecules (water19, water90 and water155). The pyrophosphate moiety in ADPR is surrounded by the β2-α7-loop and β5-α10-loop, and the latter loop

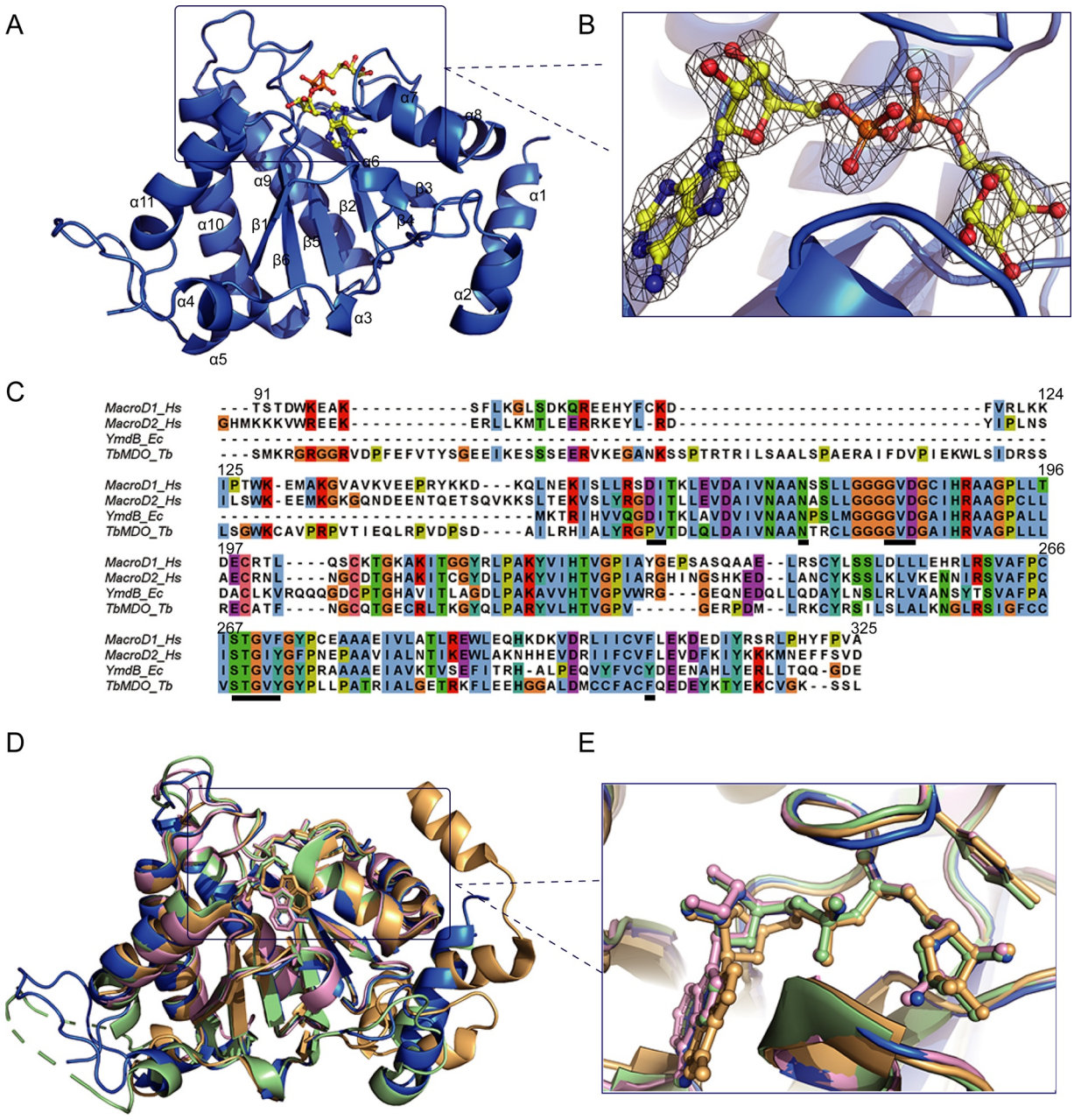

Fig. 1. Overall structure of the MacroD1-ADPR complex. (A) Marine-colored cartoon representation of the MacroD1-ADPR complex. MacroD1 exhibits the canonical three-layered α-β-α sandwich with a central six-stranded β sheet. The ADPR molecule is displayed in ball-stick with carbons in yellow. (B) 2*Fo-Fc* electron density map for ADPR contoured at 2σ (gray). (C) Sequence alignment of MacroD1_Hs, MacroD2_Hs, YmdB_Ec and TbMDO_Tb. Hs: *Homo sapiens*, Ec: *Escherichia coli*, and Tb: *Trypanosoma brucei gambiense*. The sequence alignment was generated with MAFFT and visualized using Jaview. The residues involved in ADPR binding and stabilization are underlined. (D) Structural comparison on the complexes of ADPR bound to MacroD1 homologs, including MacroD1-ADPR-Hs (marine), MacroD2-ADPR_Hs (PDB code: 4IYQ, palegreen,), YmdB-ADPR_Ec (PDB code: 5CB3, lightpink,), TbMDO-ADPR-Tb (PDB code: 5FYS, lightorange,). (E) The close-up view of ADPR in the binding pocket of the abovementioned structures. The ADPR in MacroD1-ADPR_Hs: marine ball-sticks, the ADPR in MacroD2-ADPR_Hs: palegreen ball sticks, the ADPR in YmdB-ADPR_Ec: lightpink ball-sticks, the ADPR in TbMDO-ADPR_Tb: lightorange ball sticks.

undergoes a significant conformational change upon ADPR binding (Fig. 2A). One residue (Val^{183}) from the β2-α7-loop, and four residues (Ser^{268}, Gly^{270}, Val^{271} and Phe^{272}) from β5-α10-loop are directly involved in the interaction with diphosphate group through hydrogen-bonds (Fig. 3A). The extensive network of hydrogen-bonds contributes to the majority of the binding energy of ADPR to MacroD1. The distal ribose locates to the catalytic site surrounded by the glycine-rich β2-α7-loop. Gly^{182} in the β2-α7-loop contributes to anchor the distal ribose 1″-OH group, and a hydrogen-bond network is formed between Gly^{182}, 1″-OH group of distal ribose, water12 and the α-phosphate of ADPR. Two hydrogen-bonds are formed between the 2″-OH group of distal ribose and Asn^{174} (β2-α7-loop) and Asp^{184} (helix α7) (Fig. 3A). Sequence alignment results show that the ADPR interacting residues are highly conserved in the macro domain hydrolases (Fig. 1C).

Additionally, structural comparison shows that the water12 is also conserved among the macro domain hydrolases, including the MacroD2-ADPR complex (PDB code: 4IQY), the YmdB-ADPR complex (PDB code: 5CB3) and the TbMDO-ADPR complex (PDB code: 5FSY) (Fig. 3B-E). The water12 lies close to the C1″ atom of the distal ribose with a hydrogen-bond distance of 3.1 Å. Based on the previous studies and our analysis on the MacroD1-ADPR complex, it suggests that the water12 is the catalytic water for the ADPR hydrolysis in MacroD1, and

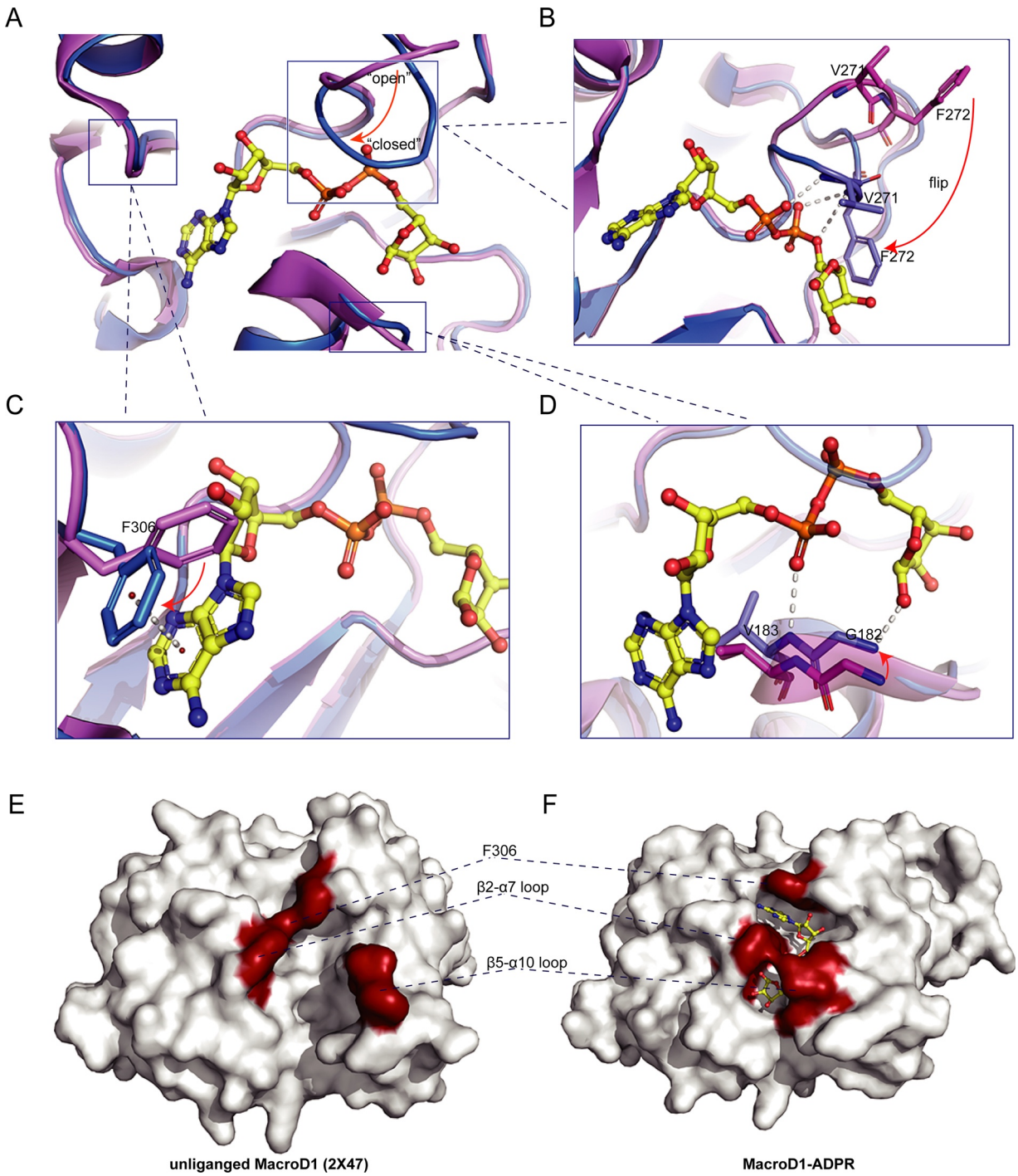

Fig. 2. Conformational change of MacroD1 upon ADPR binding. (A) Structural comparison of the apo-MacroD1 (violet) and MacroD1-ADPR complex (marine) reveals a significant conformational change in the β5-α10-loop. Additionally, two other conformational changes have been observed when ADPR binds to MacroD1. (B) Large displacement and rotation of Phe^{272} and Val^{271} in β5-α10-loop occurs upon ADPR binding. (C) Phe^{306} in the β6-α11-loop undergoes a conformational rotation and in turn contributes to π-π stacking interaction with the ADPR adenine ring. (D) Both Gly^{180} and Val^{181} in the β2-α7-loop are shifted ~ 1.3 Å to the binding pocket upon ADPR binding. (E-F) Surface representation of apo-MacroD1 (E) and MacroD1-ADPR complex (F), the significant conformational changes are highlighted in firebrick.

that the water12 will be activated and in turn launches a nucleophilic attack on the C1″ atom of the ADPR distal ribose.

In order to validate the structural analysis above, we generated 3 mutants in the ADPR binding pocket, including D160A, G182E and G182 P. The G182 P and G182E mutants introduce larger side chains, which will generate a steric hindrance and block the entrance of ADPR distal ribose, and the D160A mutant disrupts the hydrogen-bond between ADPR and MacroD1. Consequently, The D160A, G182 P and G182E mutations abolished the enzymatic activity of MacroD1-mediated ADPR hydrolysis (Fig. S1). Consistently, the results from ITC assays show that G182 P, G182E and D160A mutants cannot bind to ADPR (Fig. S2). The corresponding residue for MacroD1 Val^{271} is Ile^{189} in MacroD2, the two residues are hydrophobic amino acids and the Val^{271} main-chain, rather than its side-chain, forms a hydrogen-bond with the ADPR diphosphate group, so the V271I mutant retains the vast majority of enzymatic activity on ADPR hydrolysis (Fig. S1).

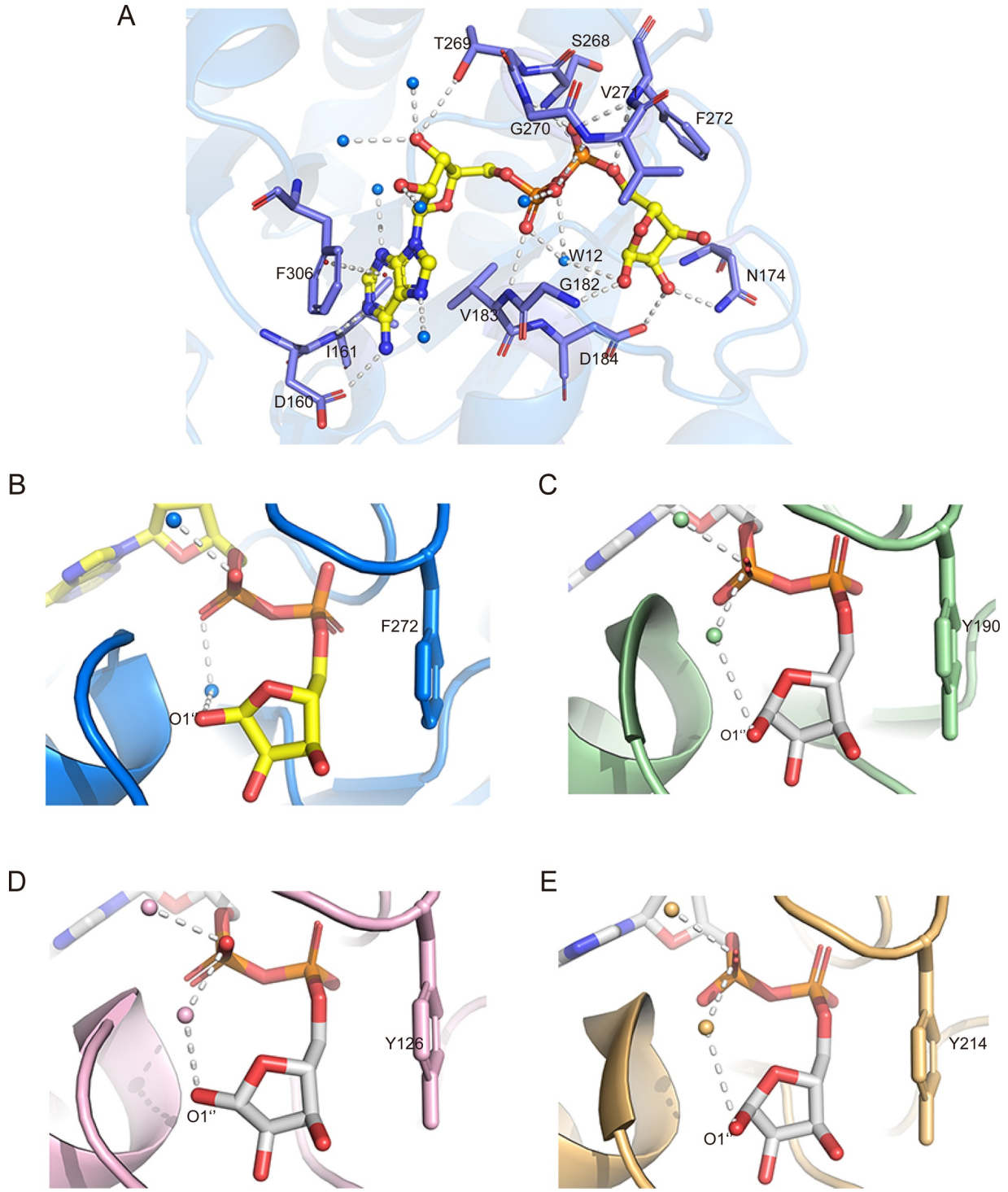

Fig. 3. Structural analysis of the ADPR-binding cavity in MacroD1. (A) The ADPR binding mode. The ADPR is in yellow ball-sticks. Residues involved in the ADPR binding are shown in marine sticks. The hydrogen bonds are in gray dashed lines. The water molecules are in blue spheres. (B-E) The coordination mode of ADPR distal ribose in diverse macro-domain hydrolases. B: MacroD1-ADPR-Hs (marine). C: MacroD2-ADPR-Hs (PDB code: 4IYQ, palegreen). D: YmdB-ADPR-Ec (PDB code: 5CB3, lightpink,). E: TbMDO-ADPR-Tb (PDB code: 5FYS, lightorange).

2.4. Catalytic mechanism of MacroD1-mediated ADPR hydrolysis

It has been suggested that Asn^{174}, Asp^{184} and His^{188} are crucial residues for MacroD1 to deacetylate OAADPr, in which Asp^{184} functions as the general base to activate the catalytic water molecule for deacetylation [21,29]. The sequence alignment results show that these catalytically relevant residues are fully conserved among the MacroD1 homologs and its paralogs (Fig. 1C). However, the D184A, N174A/D184A and D184A/H188A mutants almost retain the enzymatic activity of wild type MacroD1 on ADPR hydrolysis (Fig. 4A), indicating that these residues are not essential for the MacroD1-mediated ADPR hydrolysis. Structural analysis reveals that the distance between Asp^{184} and catalytic water12 is 4.9 Å, and there is no hydrogen-bond formed between them, indicating that Asp^{184} cannot act as the general base to activate the catalytic water12, which is in well agreement with our biochemical analyses. The function of Asp^{184} and Asn^{174} in the

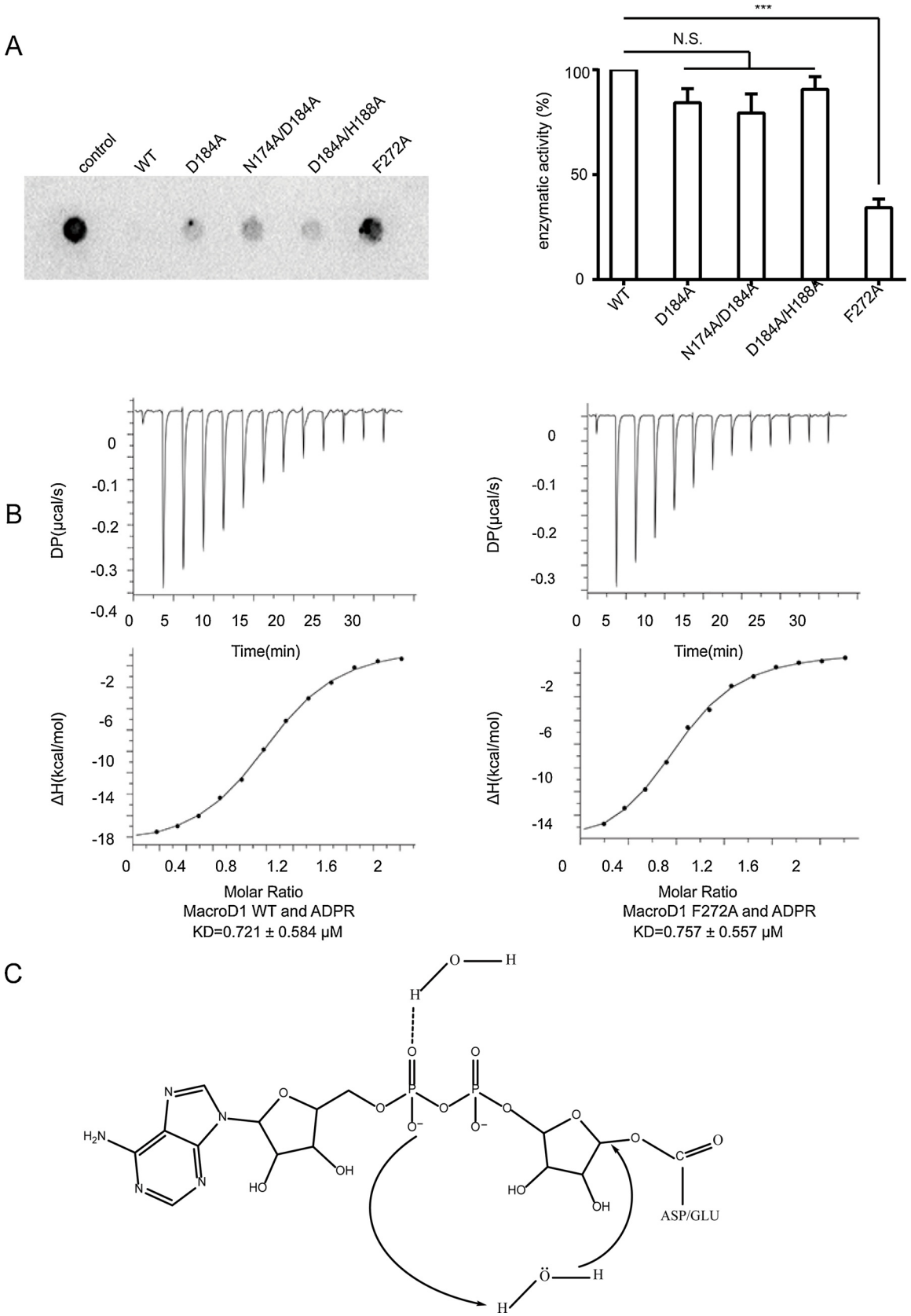

Fig. 4. Phe[272] is essential for the MacroD1-mediated ADPR hydrolysis. (A) ADPR hydrolyzation assay was carried out to measure the enzymatic activity of MacroD1 or the possible catalytic-related residue mutants. The recombinant MacroD1 or its mutants was incubated with auto-ADP ribosylation PARP10. ADPR hydrolyzation was measured by dot blotting with anti-ADPR antibody. (B) Binding affinity between ADPR and WT MacroD1/F272A mutant was measured using ITC titration. (C) A proposed mechanism for the ADPR hydrolysis from aspartate or glutamate residue acceptor.

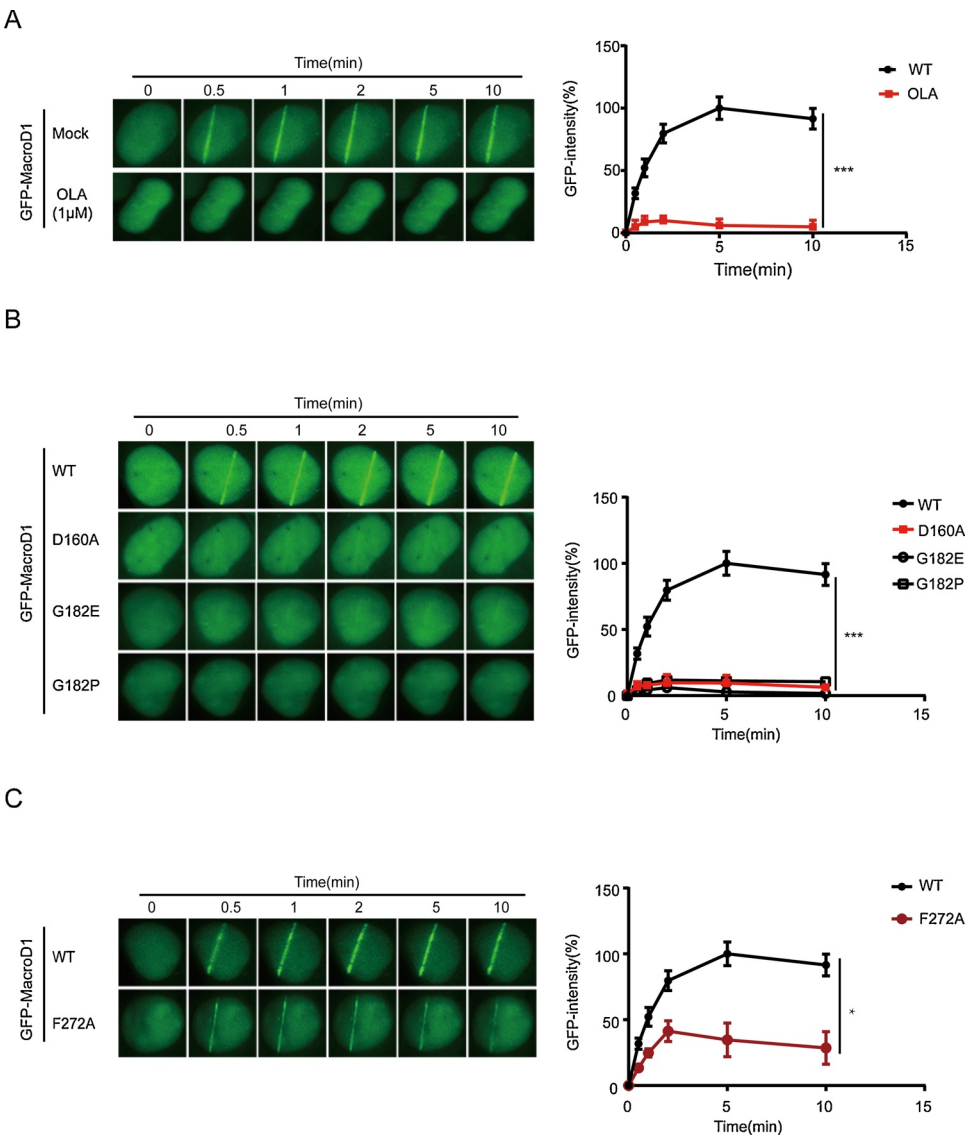

Fig. 5. The recruitment of MacroD1 to DNA lesions is mediated by ADPR recognition. (A) The recruitment of MacroD1 is mediated by ADP-ribosylation. U2OS cells expressing GFP-MacroD1 were treated with or without 1 μM olaparib. The recruitment kinetics was measured in 30 cells in three independent experiments. (B) The D160A, G182 P and G182E mutants abolish the recruitment of MacroD1 to DNA lesions. (C) The F272A mutant partially impairs the recruitment of MacroD1 to DNA lesions. The recruitment kinetics was measured in 30 cells in three independent experiments. Data are represented as mean ± s.d. as indicated from three independent experiments. *: Statistically Significant ($p < 0.05$); ***: Statistically Significant ($p < 0.001$).

MacroD1-mediated ADPR hydrolysis may be only involved in the coordination of the distal ribose in ADPR. Additionally, the distance between His^{188} and the distal ribose in ADPR is almost 7 Å, indicating that it is not involved in the catalysis of MacroD1-mediated ADPR hydrolysis, which is also consistent with our ADPR hydrolyzation assays. Combining with our structural analysis and ADPR hydrolyzation assay, it suggests that distinct catalytic residues are responsible for the MacroD1-mediated ADPR hydrolysis, rather than the catalytic residues Asn^{174}, Asp^{184} and His^{188} in the deacetylation of OAADPr.

It is observed that Phe^{272} adopts a significant conformational change in the catalytic pocket of MacroD1 upon ADPR binding, and that the corresponding phenyl group is evolutionarily conserved among macro domain hydrolases. The phenylalanine corresponding residues in MacroD2, YmdB and TbMDO are Tyr^{190}, Tyr^{126} and Tyr^{214} respectively (Fig. 1C). These aromatic residues share very similar conformational orientation, and could provide a steric hindrance for the right orientation of ADPR distal ribose in the catalytic pocket (Fig. 3B-E). As abovementioned, the ADPR molecules also adopt a similar orientation in the catalytic pocket (Fig. 1E). In contrast, the corresponding residue of Phe^{272} of MacroD1 is the Asn^{316} in MacroH2A.1.1 macro domain, which is inactive towards ADPR hydrolysis. There is no effective steric hindrance occurring owing to the residue replacement, resulting in a distinct ADPR distal ribose conformation, in which the distal ribose exhibits a more extended conformation and its C1″ atom is far away from the structurally conserved water molecule (Fig. S3). Next, we generated the F272A mutant and measured its enzymatic activity on the ADPR hydrolysis in vitro. As predicted, the F272A mutation abolishes the enzymatic activity. However, this mutant protein still retains binding affinity with ADPR (Fig. 4A and B), indicating that Phe^{272} plays an important role in the MacroD1-mediated ADPR hydrolysis, and the enzymatic activity impairment can be unrelated to the binding with ADPR. Hence, Phe^{272} is crucial for the precise orientation of distal ribose in the catalytic pocket of MacroD1.

The crystal structure of MacroD1-ADPR complex has revealed that a hydrogen-bond network is formed among Gly^{182}, 1″-OH group of the distal ribose, catalytic water12, ADPR α-phosphate, water76, and Val^{271} (Fig. 3A). This hydrogen-bond network is also observed in other macro domain hydrolases and contributes significantly to the position of catalytic water12 at the catalytic site (Fig. 3B-E). The distance between water12 and α-phosphate of ADPR is 2.7 Å, and The distance between water12 and the C1″ atom of the ADPR distal ribose is 3.1 Å. Considering the activity of ADPR α-phosphate in a polar environment and the substrate-assisted catalysis in which the functional group from a substrate is involved in the catalytic activity of its corresponding enzyme [34], it suggests that the ADPR α-phosphate functions as general base to activate water12, which induces a nucleophilic attack to the

C1″ atom of the ADPR distal ribose (Fig. 4C).

Collectively, we propose a biochemical reaction mechanism for the MacroD1-mediated ADPR hydrolysis. Upon ADPR binding, the Phe^{272} in the β5-α10-loop flips into the catalytic pocket and keeps the ADPR distal ribose in the right orientation through steric hindrance effect and dipole interaction. Meanwhile, a hydrogen-bond network, linking water12, ADPR α-phosphate and other elements, is responsible for the precise position of water12 in the catalytic pocket. The water12 is then activated by the ADPR α-phosphate and induces a nucleophilic attack to the distal ribose C1″ atom of ADPR, cleaving the glycosidic bond between the distal ribose C1″ atom and the acceptor Asp/Glu residue. The significance of ADPR α-phosphate and the catalytic water in the MacroD2-mediated ADPR hydrolysis have been reported by Gytis Jankevicius et al. [22]. Collectively, the evolutionarily conserved aromatic residue, structurally conserved catalytic water and the same conformation of ADPR in the catalytic pocket suggest that the MacroD-like macro domain hydrolases may use the same catalytic mechanism for the ADPR hydrolysis.

2.5. The enzymatic activity of MacroD1 plays an important role in DNA damage repair

ADPR hydrolases are known to regulate DNA damage repair. Although MacroD1 is reported to exist in mitochondria, it has been shown that similar to its paralog MacroD2, at least a small amount of MacroD1 localizes in nucleus, particularly relocalizes to nucleus in response to cellular stress [9,22]. Using laser microirradiation assays, we examined the recruitment of MacroD1 to DNA lesions. MacroD1 was recruited to the DNA lesions within 30 s following laser-induced DNA damage, and this relocation process was suppressed by the PARP inhibitor olaparib treatment (Fig. 5A), suggesting that the recruitment of MacroD1 to DNA lesions is mediated by DNA damage-induced ADP-ribosylation. Compared to wild type MacroD1, D160A, G182 P and G182E mutants failed to relocate to DNA lesions since these mutants disrupted the ADPR-binding pocket, indicating that ADPR recognition plays a key role for the recruitment of MacroD1 to DNA damage site (Fig. 5B). Interestingly, the F272A mutant was still recruited to DNA damage site (Fig. 5C), suggesting that the catalytic-related residue is not required for the recruitment of MacroD1 to DNA damage site. Thus, these results reveal that ADPR recognition is essential for the recruitment of MacroD1 to DNA damage sites.

Next, to examine the role of MacroD1 in DNA damage repair, we knocked down the endogenous MacroD1 with siRNA, and expressed wild type MacroD1 and its mutants in U2OS cells (Fig. 6A). The transfected cells were treated with methyl methanesulfonate (MMS), a DNA damaging reagent. The DNA damage repair kinetics was measured using comet assays. Under both neutral and alkaline conditions, the DNA damage repair was impaired once cells were only expressing MacroD1 mutants (Fig. 6B and C), suggesting that MacroD1-mediated ADPR hydrolyzation plays a crucial role in DNA damage repair.

3. Discussion

In this study, we have solved the structure of the MacroD1-ADPR complex, which allows us to dissect the molecular mechanism of MacroD1-mediated ADPR hydrolysis. Although the crystal structure of apo-MacroD1 has been solved [21], the true catalytic residues for the ADPR hydrolysis were unclear until this study. With the structure of apo-MacroD1 and additional modeling analysis, 11 individual residues were mutated, including Asp^{160}, Asp^{167}, Asn^{171}, Asn^{174}, Ser^{176}, Asp^{184} His^{188}, Thr^{226}, Ser^{268}, Gly^{270} and Cys^{299}, to examine their roles in the enzymatic activity of MacroD1-mediated deacetylation of OAADPr [21]. The mutational analyses indicated a catalytic role for Asn^{174}, Asp^{184} and His^{188} in the deacetylation of OAADPr, which was further validated by Brett M. Hirsch et al. [29]. They proposed that Asp^{184} works as a general base to deprotonate the catalytic water, which further launches an nucleophilic attack on the carbonyl group, resulting in the hydrolyzation of the acetyl group from OAADPr.

In this study, compared with apo-MacroD1, our structure of MacroD1-ADPR complex reveals the conformational plasticity of β5-α10-loop, which exists in open and closed conformational states. A structural rearrangement, required for the specific substrate recognition, is observed upon ADPR binding (Fig. 2). Additionally, the structural conserved water (water12) is observed in the catalytic site of MacroD1, which also existed in other MacroD-like proteins (Fig. 3). Structural analysis in the catalytic site of MacroD1 is listed as follows: [1] Asn^{174} and Asp^{184} work together to coordinate the 2″-OH group of distal ribose; [2] the distance between catalytic water12 and Asp^{184} is 4.9 Å, and there is no hydrogen-bond between them, [3] the distance between His^{188} and the distal ribose in ADPR is almost 7 Å. Our structural analysis may indicate that the catalytic residues for the MacroD1-mediated ADPR hydrolysis are different from that of deacetylation of OAADPr, which is further validated in the ADPR hydrolyzation assays. The D184A, N174A/D184A and D184A/H188A mutants almost retain full enzymatic activity on ADPR hydrolysis, indicating that other residues are involved in the ADPR hydrolysis. Indeed, the indirect roles of Asn^{174} and Asp^{184} in the MacroD1-mediated ADPR hydrolysis have also been revealed by Ladurner *et al*, and their results show that the N174A/D184A mutant retains strong activity toward PARP10 [22].

It's noteworthy that Phe^{272} from β5-α10-loop exhibits a significant conformational change upon ADPR binding. Although the F272A mutant has little effect on ADPR binding, it almost abolished the enzymatic activity of ADPR hydrolysis (Fig. 4A), indicating that Phe^{272} plays a crucial role in ADPR hydrolysis. Sequence alignment shows that the phenyl group from Phe^{272} is evolutionary conserved among macro domain hydrolases. Furthermore, structural alignment reveals that conformation of Phe^{272} in MacroD1-ADPR complex is very similar to the corresponding residues in other macro domain hydrolases, including Tyr^{190} in MacroD2-ADPR complex (PDB code: 4IQY), Tyr^{126} in YmdB-ADPR complex (PDB code: 5CB3) and Tyr^{214} in TbMDO-ADPR complex (PDB code: 5FSY) (Fig. 3B-E). Additionally, their ADPR molecules adopt a similar conformation. Interestingly, several strains of virus, such as coronaviruses, also contain MacroD-like domains that retain the conserved Phe residues at the similar positions (Fig. S4), suggesting that these macro domains may also regulates ADPR hydrolysis during viral infection [35–37]. Both evolutionary conservation and conformational similarity of the phenyl group indicate that the significance of aromatic residues in the ADPR hydrolysis. In contrast, the structure of ADPR bound to the MacroH2A1.1 macro domain (inactive) reveals that the corresponding residue for MacroD1 Phe^{272} is Asn^{316}, and the disappearance of steric hindrance, which is generated by phenyl group, makes the distal ribose in a relatively extended conformation, in which its C1″ atom is far away from the catalytic water (Fig. S3) [38]. It is assumed that the presence of phenyl group plays a significant role in catalysis process. Indeed, it has been reported that the YmdB Y126A mutation completely abolishes the enzymatic activity on ADPR hydrolysis, whereas Y126 F mutant had little impact on its enzymatic activity [28]. Taken together, it is suggested that the evolutionally conserved phenyl group from aromatic amino acid plays an important role on the ADPR hydrolysis, Phe^{272} can provide the right orientation and stabilization of ADPR distal ribose in the catalytic site. More importantly, it seems that it is an efficient evolution strategy to replace a single amino acid to make the catalytic components in right orientation to complete the desired function.

Structure comparison also reveals that a hydrogen-bond network, linking the catalytic water, ADPR α-phosphate and other residues, is conserved in the macro domain hydrolases (Fig. 3B-E). The common hydrogen-bond network contributes significantly to hold and orient catalytic water in the catalytic site. Both structural analysis and biochemical analysis have shown that Asp^{184} cannot work as the general base to activate the catalytic water at the process of ADPR hydrolysis.

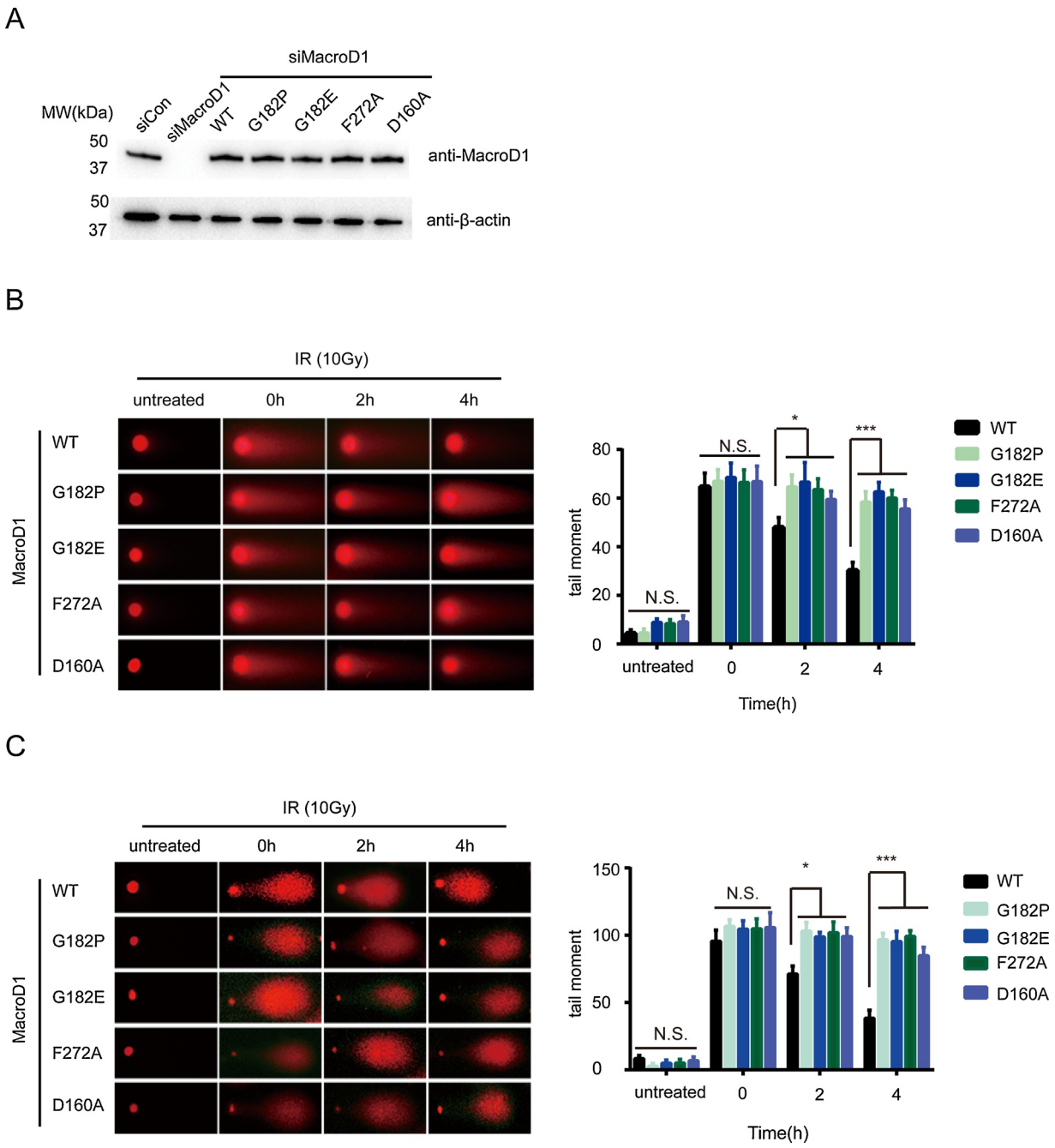

Fig. 6. Enzymatic activity of MacroD1 plays an important role for DNA damage repair. (A) U2OS cells were expressing the MacroD1 mutants. U2OS cells were treated with siRNA to knock down the endogenous MacroD1, and the cells were expressing wild type MacroD1 or its mutants. Comet assays were carried out under either neutral (B) or alkaline conditions (C). Comet tail moments were measured to indicate the DNA damage repair kinetics. Data are represented as mean ± s.d. as indicated from three independent experiments. *: Statistically Significant ($p < 0.05$); ***: Statistically Significant ($p < 0.001$).

The absence of a residue to activate catalytic water in the catalytic site and the substrate-assisted catalysis mechanism allow us to surmise that the ADPR α-phosphate works as the general base to activate the catalytic water12, which further carries on a nucleophilic attack on the distal ribose C1″ atom. The phenomenon that the involvement of a substrate phosphate as a general base in the enzymatic activity has been observed in many other enzymes, such as restriction endonucleases, aminoacyl tRNA syanthetases, RNase HI, aspartate carbamoyl-transferase, and so on [34].

In addition to the structural and biochemical analysis, we further explored the roles of abovementioned residues in the MacroD1-mediated DNA damage repair. Laser microirradiation assays revealed that MacroD1 is recruited to DNA lesions, which is mediated by DNA damage-induced PARylation (Fig. 5A). The ADPR binding residues are required for the recruitment of MacroD1 to DNA lesions (Fig. 5B). However, Phe^{272}, although very important for catalytic activity of ADPR hydrolysis, is not necessary for the recruitment of MacroD1 to DNA damage site, indicating that the catalytic-related residue is not responsible for the recruitment of MacroD1 to DNA lesions (Fig. 5C). Furthermore, due to the lack of enzymatic activity, the MacroD1 mutants abolished the MacroD1-mediated DNA damage repair (Fig. 6).

Accumulated evidence suggests that ADP-ribosylation mediates the recruitment of DNA damage repair factors to the DNA damage sites for lesion repair, and deADP-ribosylation is a sequential step to remove ADP-ribosylation and facilitates repair. If deADP-ribosylation is abolished, these DNA damage repair factors will be trapped at DNA lesions

Table 1
Data collection and refinement statistics of MacroD1-ADPR complex.

	MacroD1-ADPR
Data collection	
Space group	P1211
Cell dimensions	
a, *b*, *c* (Å)	79.9, 106.2, 79.9
α, β, γ (°)	90.0, 120.0, 90.0
Wavelength (Å)	0.9791
Resolution (Å)	32.9 − 2.0 (2.071 − 2.0)[a]
R_{merge}(%)	4.6 (57.3)
$\langle I/\sigma(I)\rangle$	13.12 (1.68)
Redundancy	1.89 (1.9)
Refinement	
Resolution (Å)	32.9 − 2.0
No. reflections	75848
R_{work} / R_{free} (%)	24.0/28.3
No. atoms	
Protein	7408
ADPR	144
Water	416
B-factors	
Protein	48.11
ADPR	43.66
Water	45.03
R.m.s deviations	
Bond lengths (Å)	0.008
Bond angles (°)	0.982

[a] Statistics for the highest-resolution shell are shown in parentheses.

by ADP-ribosylation and impair DNA damage repair [7,8]. It has been shown that dePARylation plays a key role in DNA damage repair [8,30]. Consistently, we found that lacking MacroD1 also impaired DNA damage repair. In addition to MacroD1, PARG is another potent enzyme to remove PARylation during DNA damage repair. However, it cannot remove the last ADPR unit linked to the targeted proteins. In contrast, MacroD1 is able to remove the terminal ADPR unit from the targeted proteins. Thus, PARG and MacroD1 may function together to erase PARylation at DNA lesions and facilitate DNA damage repair. Moreover, MacroD1 is only one of the ADP-ribosylhydrolases, and may have redundant role with other ADP-ribosylhydrolases such as TARG1 and MacroD2. Thus, we did not observe the increased cellular sensitivity to DNA damaging agents when cells were lacking MacroD1. In addition to the nuclear MacroD1, it can also be imported into mitochondria. Following the relocation, the N-terminal 77 residues are cleaved, thus generating an N-terminal truncated isoform. It remains intriguing if mitochondrial MacroD1 plays a role in DNA damage repair in mitochondria. Since the folding of Macrodomain is not affected by the cleavage, the mitochondrial isoform should retain the enzymatic activity. Since heavy oxidative damage always occurs in mitochondria, it is possible that MacroD1 may regulate oxidative damage repair in mitochondria. The functional significance of MacroD1 in DNA damage repair in mitochrondia should be further examined in future.

In summary, our study provides mechanistic insights into the MacroD1-mediated ADPR hydrolysis, which may explain its biological functions in cellular processes such as DNA damage repair.

4. Experimental procedures

4.1. Protein expression and purification

The DNA sequence encoding Human MacroD1 was amplified from a 293 T cDNA library. The amplified PCR product was digested with *BamH*I and *Xho*I, and then was constructed into the modified pET-15b vector, generating the recombinant MacroD1 with a hexahistidine tag fusion at the N-terminus for protein expression and purification. The N-terminal 90 residues of MacroD1 were removed at the process of cloning. The full length MacroD1 was also generated and used in all other experiments, rather than the Crystallization.

Escherichia coli Rosetta (DE3) carrying the recombinant plasmid was cultured in L Broth media supplemented with 100 μg/mL ampicillin and 34 μg/mL chloramphenicol at 37 °C. When the bacterial density reached to the OD_{600} of 0.8–1.0, the growing temperature was drop to 16 °C, and isopropyl β-D-1-thiogalactopyranoside (IPTG), at final concentration of 0.1 mM, was added to induce recombinant protein expression for 12 h. Cells were harvested by centrifugation and then resuspended in ice-cold lysis-buffer (20 mM Tris-HCl pH 8.0, 500 mM NaCl). The cells were lysed by sonication and centrifuged (30,000 *g*, 50 min) to obtain the supernatant containing soluble MacroD1.

For protein purification, the supernatant was loaded onto a Ni-chelating Sepharose column (GE Healthcare) which was pre-equilibrated with lysis-buffer. After extensively washing with wash-buffer (20 mM Tris-HCl pH 8.0, 500 mM NaCl, 50 mM imidazole), the soluble MacroD1 was eluted using elution-buffer (20 mM Tris-HCl pH 8.0, 500 mM NaCl, 300 mM imidazole). The elutes were further purified using Superdex 75 column (GE Healthcare) in 20 mM Tris-HCl pH 8.0, 150 mM NaCl and 1 mM DTT. The MacroD1 mutant proteins are purified using the same protocol.

4.2. Crystallization and data collection

To screen the MacroD1-ADPR complex, MacroD1 and ADPR (Sigma) were mixed in the molar ratio of 1:3. Preliminary crystallization was performed using the sitting-drop vapor-diffusion method at 18 °C by mixing equal volumes of reservoir solution and MacroD1-ADPR complex. After optimization, the best crystals of MacroD1-ADPR complex were obtained using a reservoir solution consisting of 0.2 M Sodium thiocyanate, 20 % PEG 3350. For X-ray data collection, the Crystals were soaked in the cryoprotectant buffer containing reservoir solution supplemented with 20 % glycerol (v/v), and then flash-cooled in liquid nitrogen.

Crystal diffraction data were collected at Shanghai Synchrotron Radiation facility (SSRF), beamline BL19U. The crystal belongs to space group P1121 with the unit cell dimensions a =79.9 Å, b =106.2 Å, c =79.9 Å, and β = 120.00°. The data set was processed with XDS [39].

4.3. Structure determination and refinement

The crystal structure of MacroD1-ADPR complex was determined through molecular replacement using PHASER from the CCP4 software package [40]. The structure of apo-MacroD1 (PDB code: 2X47) was used as the search model. COOT [41] and PHENIX [42] were used repeatedly for manual model building and refinement. The data collection and refinement statistics are summarized in Table 1. All the molecular graphics figures are prepared using PyMol (http://www.pymol.org).

4.4. Cell culture

U2OS cells were maintained in DMEM medium with 10 % fetal bovine serum and cultivated at 37 °C in 5 % CO2 (v/v). U2OS cells were transfected with plasmids encoding MacroD1 or its mutants.

4.5. Plasmids and siRNA

Human MacroD1 and its mutants were cloned into pEGFP-C1, pET-15b, and pCDNA3 vectors. Human PARP10 full-length cDNA was cloned to the pGEX-4T-1 vector. MacroD1 siRNA targeting sequence was 5′ - GGAGCCCAGGUAUAAAAAGUU-3′.

4.6. Laser microirradiation and microscope image acquisition

The transfected U2OS Cells with GFP-tagged corresponding

plasmids were plated on 35-mm glass bottom dishes (NEST Biotechnology). Laser microirradiation was carried out using OLYMPUS IX71 inverted fluorescence microscope combined with the MicroPoint Laser Illumination and Ablation System (Photonic Instruments, Inc.). The pulse energy is 170 microjoules at 10 Hz, and the exposure time of cell to the laser beam is about 3.5 ns. The images were taken using the same microscope and further processed by the CellSens software (Olympus). The GPF fluorescence strips was measured at the indicated time points and further analyzed using Image J software. 30 cells were analyzed from three independent experiments. Error bars represent the standard deviation.

4.7. Comet assay

We performed single-cell gel electrophoretic comet assay to detect single strand DNA breaks under alkaline condition and DNA double strand breaks under neutral conditions. U2OS cells were recovered in normal culture medium for a certain period of time with or without the indicated treatment. Cells were collected and washed twice with ice-cold PBS; 2×10^4/mL cells were mixed with 1 % LMAgarose at a ratio of 1:3 (v/v) at 40 ˚C, and immediately pipetted onto slides. The slides were immersed in alkaline lysis solution (1.2 M NaCl, 260 mM NaOH, 100 mM EDTA, 0.1 % sarkosyl), followed by washing in the rinse buffer (90 mM Tris-HCl pH 8.5, 90 mM boric acid, 2 mM EDTA) and alkaline wash buffer (30 mM NaOH, 2 mM EDTA) with two repeats for 30 min. The slides were then subjected to electrophoresis at 20 V (0.6 V/cm) for 30 min and stained in 2.5 μg/mL propidium iodide for 25 min. All images were taken by fluorescence microscope and analyzed by Comet Assay IV software.

4.8. Auto-ADP-ribosylation of PARP10

The auto-ADP-ribosylation of PARP10 was used as the substrate of MacroD1 in the ADPR hydrolysis assay and prepared using the previously published methods [31]. The PARP10 auto-ADP-ribosylation was carried out in a 100 μl reaction system consisting of 10 mM Tris-HCl pH 8.0, 10 mM DTT and 10 mM $MgCl_2$ and 10 ng GST-PARP10 and 5 μM NAD^+ (Sigma). The auto-modification reaction was carried out at 37 ˚C for 30 min. And then the auto-modified PARP10 was purified using Glutathione Sepharose from the reaction buffer. The aliquot 10 μL to 10 tubes.

4.9. ADPR hydrolyzation assay

Approximately 10 μL auto-modified PARP10 protein and 0.5 μM each recombination protein mixed well and reacted at 37 ˚C for 60 min. Then, the reaction mixture was heated at 95 ˚C for 5 min, and 2 μL samples were dotted onto the nitrocellulose membranes. The dot blotting assays were carried out using anti-ADPR antibody (Cell Signaling Technology).

4.10. Isothermal titration calorimetry

Isothermal titration binding assays were performed at 25 ˚C using PEAQ-ITC instrument (MALvern). Binding reactions were carried out in 20 mM Tris-HCl pH 8.0 and 150 mM NaCl. MacroD1 (or its mutants, 20–30 μM) and ADPR (200–400 μM) were loaded in Sample Cell and Titration Syringe respectively. The titration protocol consists of 0.4 μl pre-injection and sequential 12 × 2 μL injections at 200 s intervals.

Accession code

The atomic coordinates and structure factors for the MacroD1-ADPR complex have been deposited in the Protein Data Bank with the Accession Code 6LH4.

Author contributions

X.Y. performed the experiments and wrote the manuscript. Y.M., Y.L. and Y.D. performed the experiments and analyzed the data. L.Y., H.W. and L.G. performed the experiments. X.Y., C.W. and X.L. designed the project, analyzed the data and wrote the manuscript.

Declaration of Competing Interest

All the authors declare no conflict of interest.

Acknowledgements

The authors thank the beamline BL19U staff at the Shanghai Synchrotron Radiation facility for X-ray data collection experiments. This work was supported by the National Natural Science Foundation of China (Grant No. 81672794 and 31670812), Ministry of Education ChunHui Project (Grant No. 23), Foundation of Hebei Educational committee (Grant No. ZD2020183), Natural Science Foundation of Hebei province (No. C2018201171), Hebei Province Foundation for Returned Overseas Chinese Scholars and research funds from Westlake University.

Appendix A. Supplementary data

Supplementary data associated with this article can be found, in the online version, at doi:https://doi.org/10.1016/j.dnarep.2020.102899.

References

[1] P. Bai, Biology of poly(ADP-Ribose) polymerases: the factotums of cell maintenance, Mol. Cell 58 (2015) 947–958.
[2] E. Barkauskaite, G. Jankevicius, I. Ahel, Structures and mechanisms of enzymes employed in the synthesis and degradation of PARP-Dependent protein ADP-Ribosylation, Mol. Cell 58 (2015) 935–946.
[3] J.C. Ame, C. Spenlehauer, G. de Murcia, The PARP superfamily, Bioessays 26 (2004) 882–893.
[4] D. Corda, M. Di Girolamo, Functional aspects of protein mono-ADP-ribosylation, EMBO J. 22 (2003) 1953–1958.
[5] A.K. Leung, Poly(ADP-ribose): an organizer of cellular architecture, J. Cell Biol. 205 (2014) 613–619.
[6] S. Vyas, I. Matic, L. Uchima, J. Rood, R. Zaja, R.T. Hay, I. Ahel, P. Chang, Family-wide analysis of poly(ADP-ribose) polymerase activity, Nat. Commun. 5 (2014) 4426.
[7] C. Liu, A. Vyas, M.A. Kassab, A.K. Singh, X. Yu, The role of poly ADP-ribosylation in the first wave of DNA damage response, Nucleic Acids Res. 45 (2017) 8129–8141.
[8] M.A. Kassab, X. Yu, The role of dePARylation in DNA damage repair and cancer suppression, DNA Repair (Amst) 76 (2019) 20–29.
[9] T. Agnew, D. Munnur, K. Crawford, L. Palazzo, A. Mikoc, I. Ahel, MacroD1 is a promiscuous ADP-Ribosyl hydrolase localized to mitochondria, Front. Microbiol. 9 (2018) 20.
[10] S. Oka, J. Kato, J. Moss, Identification and characterization of a mammalian 39-kDa poly(ADP-ribose) glycohydrolase, J. Biol. Chem. 281 (2006) 705–713.
[11] T. Ono, A. Kasamatsu, S. Oka, J. Moss, The 39-kDa poly(ADP-ribose) glycohydrolase ARH3 hydrolyzes O-acetyl-ADP-ribose, a product of the Sir2 family of acetyl-histone deacetylases, Proc. Natl. Acad. Sci. U. S. A. 103 (2006) 16687–16691.
[12] P. Fontana, J.J. Bonfiglio, L. Palazzo, E. Bartlett, I. Matic, I. Ahel, Serine ADP-ribosylation reversal by the hydrolase ARH3, Elife 6 (2017).
[13] J. Moss, M.K. Jacobson, S.J. Stanley, Reversibility of arginine-specific mono(ADP-ribosyl)ation: identification in erythrocytes of an ADP-ribose-L-arginine cleavage enzyme, Proc. Natl. Acad. Sci. U. S. A. 82 (1985) 5603–5607.
[14] W. Han, X. Li, X. Fu, The macro domain protein family: structure, functions, and their potential therapeutic implications, Mutat. Res. 727 (2011) 86–103.
[15] G.I. Karras, G. Kustatscher, H.R. Buhecha, M.D. Allen, C. Pugieux, F. Sait, M. Bycroft, A.G. Ladurner, The macro domain is an ADP-ribose binding module, EMBO J. 24 (2005) 1911–1920.
[16] J.G. Rack, D. Perina, I. Ahel, Macrodomains: structure, function, evolution, and catalytic activities, Annu. Rev. Biochem. 85 (2016) 431–454.
[17] R. Alvarez-Gonzalez, F.R. Althaus, Poly(ADP-ribose) catabolism in mammalian cells exposed to DNA-damaging agents, Mutat. Res. 218 (1989) 67–74.
[18] E. Barkauskaite, G. Jankevicius, A.G. Ladurner, I. Ahel, G. Timinszky, The recognition and removal of cellular poly(ADP-ribose) signals, FEBS J. 280 (2013) 3491–3507.
[19] W. Lin, J.C. Ame, N. Aboul-Ela, E.L. Jacobson, M.K. Jacobson, Isolation and characterization of the cDNA encoding bovine poly(ADP-ribose) glycohydrolase, J. Biol. Chem. 272 (1997) 11895–11901.

[20] D. Slade, M.S. Dunstan, E. Barkauskaite, R. Weston, P. Lafite, N. Dixon, M. Ahel, D. Leys, I. Ahel, The structure and catalytic mechanism of a poly(ADP-ribose) glycohydrolase, Nature 477 (2011) 616–620.
[21] D. Chen, M. Vollmar, M.N. Rossi, C. Phillips, R. Kraehenbuehl, D. Slade, P.V. Mehrotra, F. von Delft, S.K. Crosthwaite, O. Gileadi, J.M. Denu, I. Ahel, Identification of macrodomain proteins as novel O-acetyl-ADP-ribose deacetylases, J. Biol. Chem. 286 (2011) 13261–13271.
[22] G. Jankevicius, M. Hassler, B. Golia, V. Rybin, M. Zacharias, G. Timinszky, A.G. Ladurner, A family of macrodomain proteins reverses cellular mono-ADP-ribosylation, Nat. Struct. Mol. Biol. 20 (2013) 508–514.
[23] F.C. Peterson, D. Chen, B.L. Lytle, M.N. Rossi, I. Ahel, J.M. Denu, B.F. Volkman, Orphan macrodomain protein (human C6orf130) is an O-acyl-ADP-ribose deacylase: solution structure and catalytic properties, J. Biol. Chem. 286 (2011) 35955–35965.
[24] J.G.M. Rack, A. Ariza, B.S. Drown, C. Henfrey, E. Bartlett, T. Shirai, P.J. Hergenrother, I. Ahel, (ADP-ribosyl)hydrolases: structural basis for differential substrate recognition and inhibition, Cell Chem. Biol. 25 (2018) 1533–1546 e1512.
[25] F. Rosenthal, K.L. Feijs, E. Frugier, M. Bonalli, A.H. Forst, R. Imhof, H.C. Winkler, D. Fischer, A. Caflisch, P.O. Hassa, B. Luscher, M.O. Hottiger, Macrodomain-containing proteins are new mono-ADP-ribosylhydrolases, Nat. Struct. Mol. Biol. 20 (2013) 502–507.
[26] R. Sharifi, R. Morra, C.D. Appel, M. Tallis, B. Chioza, G. Jankevicius, M.A. Simpson, I. Matic, E. Ozkan, B. Golia, M.J. Schellenberg, R. Weston, J.G. Williams, M.N. Rossi, H. Galehdari, J. Krahn, A. Wan, R.C. Trembath, A.H. Crosby, D. Ahel, R. Hay, A.G. Ladurner, G. Timinszky, R.S. Williams, I. Ahel, Deficiency of terminal ADP-ribose protein glycohydrolase TARG1/C6orf130 in neurodegenerative disease, EMBO J. 32 (2013) 1225–1237.
[27] T. Haikarainen, L. Lehtio, Proximal ADP-ribose hydrolysis in Trypanosomatids is catalyzed by a macrodomain, Sci. Rep. 6 (2016) 24213.
[28] W. Zhang, C. Wang, Y. Song, C. Shao, X. Zhang, J. Zang, Structural insights into the mechanism of Escherichia coli YmdB: a 2'-O-acetyl-ADP-ribose deacetylase, J. Struct. Biol. 192 (2015) 478–486.
[29] B.M. Hirsch, E.S. Burgos, V.L. Schramm, Transition-state analysis of 2-O-acetyl-ADP-ribose hydrolysis by human macrodomain 1, ACS Chem. Biol. 9 (2014) 2255–2262.
[30] M.A. Kassab, L.L. Yu, X. Yu, Targeting dePARylation for cancer therapy, Cell Biosci. 10 (2020) 7.
[31] S.H. Chen, X. Yu, Targeting dePARylation selectively suppresses DNA repair-defective and PARP inhibitor-resistant malignancies, Sci. Adv. 5 (2019) eaav4340.
[32] M. Neuvonen, T. Ahola, Differential activities of cellular and viral macro domain proteins in binding of ADP-ribose metabolites, J. Mol. Biol. 385 (2009) 212–225.
[33] M. Wang, Z. Yuan, R. Xie, Y. Ma, X. Liu, X. Yu, Structure-function analyses reveal the mechanism of the ARH3-dependent hydrolysis of ADP-ribosylation, J. Biol. Chem. 293 (2018) 14470–14480.
[34] W. Dall'Acqua, P. Carter, Substrate-assisted catalysis: molecular basis and biological significance, Protein Sci. 9 (2000) 1–9.
[35] M.P. Egloff, H. Malet, A. Putics, M. Heinonen, H. Dutartre, A. Frangeul, A. Gruez, V. Campanacci, C. Cambillau, J. Ziebuhr, T. Ahola, B. Canard, Structural and functional basis for ADP-ribose and poly(ADP-ribose) binding by viral macro domains, J. Virol. 80 (2006) 8493–8502.
[36] Y. Xu, L. Cong, C. Chen, L. Wei, Q. Zhao, X. Xu, Y. Ma, M. Bartlam, Z. Rao, Crystal structures of two coronavirus ADP-ribose-1"-monophosphatases and their complexes with ADP-Ribose: a systematic structural analysis of the viral ADRP domain, J. Virol. 83 (2009) 1083–1092.
[37] C.C. Cho, M.H. Lin, C.Y. Chuang, C.H. Hsu, Macro domain from middle east respiratory syndrome coronavirus (MERS-CoV) is an efficient ADP-ribose binding module: CRYSTAL STRUCTURE AND BIOCHEMICAL STUDIES, J. Biol. Chem. 291 (2016) 4894–4902.
[38] G. Timinszky, S. Till, P.O. Hassa, M. Hothorn, G. Kustatscher, B. Nijmeijer, J. Colombelli, M. Altmeyer, E.H. Stelzer, K. Scheffzek, M.O. Hottiger, A.G. Ladurner, A macrodomain-containing histone rearranges chromatin upon sensing PARP1 activation, Nat. Struct. Mol. Biol. 16 (2009) 923–929.
[39] W. Kabsch, Xds, Acta Crystallogr. D Biol. Crystallogr. 66 (2010) 125–132.
[40] A.J. McCoy, R.W. Grosse-Kunstleve, P.D. Adams, M.D. Winn, L.C. Storoni, R.J. Read, Phaser crystallographic software, J. Appl. Crystallogr. 40 (2007) 658–674.
[41] P. Emsley, B. Lohkamp, W.G. Scott, K. Cowtan, Features and development of coot, Acta Crystallogr. D Biol. Crystallogr. 66 (2010) 486–501.
[42] P.D. Adams, P.V. Afonine, G. Bunkoczi, V.B. Chen, I.W. Davis, N. Echols, J.J. Headd, L.W. Hung, G.J. Kapral, R.W. Grosse-Kunstleve, A.J. McCoy, N.W. Moriarty, R. Oeffner, R.J. Read, D.C. Richardson, J.S. Richardson, T.C. Terwilliger, P.H. Zwart, PHENIX: a comprehensive Python-based system for macromolecular structure solution, Acta Crystallogr. D Biol. Crystallogr. 66 (2010) 213–221.